AJNR

MR imaging of cerebral vascular malformations.

B C Lee, L Herzberg, R D Zimmerman and M D Deck

AJNR Am J Neuroradiol 1985, 6 (6) 863-870
http://www.ajnr.org/content/6/6/863

MR Imaging of Cerebral Vascular Malformations

Benjamin C. P. Lee[1,2]
Louis Herzberg[1]
Robert D. Zimmerman[1]
Michael D. F. Deck[1]

Fifteen vascular malformations, including six supratentorial arteriovenous malformations (AVMs), three venous malformations, and six brainstem vascular malformations, were examined on 0.5 T magnetic resonance (MR) and GE 9800 and 8800 computed tomographic (CT) scanners. All the malformations were shown by MR, and the arterial and venous drainage of AVMs was precisely delineated. Hematoma was always differentiated from calcification by MR signal characteristics. Increased signal in the brain parenchyma was often seen adjacent to AVMs. The signal of blood within venous malformations altered with spin-echo techniques using various repetition times and was distinguished from rapidly flowing blood in AVMs that lacked signal in all imaging sequences. Brainstem malformations were seldom demonstrated by angiography. Hemorrhage was common and was invariably associated with multiple areas of absent signal that may have represented abnormal vessels. These appearances are distinct from those of intrinsic tumors and are probably pathognomonic of brainstem vascular malformations.

Vascular malformations present clinically with a variety of symptoms that include subarachnoid hemorrhage, seizures, and focal neurologic deficits [1, 2]. Computed tomography (CT) demonstrates the abnormal vessels and hemorrhages associated with the malformations [3, 4]. Treatment depends on the histologic type, anatomic location, and size of the vascular malformations, as well as the clinical status of the patient [4–12]. Lesions situated in the dominant hemisphere; in important functional locations such as the speech, motor, and sensory centers; as well as those in the thalamus and brainstem are seldom amenable to curative surgical excision [13]. Malformations smaller than 1 cm may be treated by proton beam therapy [14]. Very accurate localization of the malformation is useful for surgical therapy and essential for radiotherapy to avoid damage to adjacent normal brain tissue.

The major advantages of magnetic resonance (MR) imaging over CT are the absence of bone artifact, sensitivity in detecting subtle contrast differences between normal and abnormal tissue, and ability to differentiate hematoma from most calcified lesions [15, 16]. Direct sagittal views provide an additional perspective in localization. It may also be possible, by using different imaging sequences, to define flow characteristics within the malformations [17, 18]. This report compares MR with CT in the diagnosis and evaluation of intracerebral vascular malformations.

Subjects and Methods

Fifteen vascular malformations were demonstrated in 14 patients. The malformations were supratentorial in seven cases, infratentorial in six, and in both locations in one.

MR scans were obtained using a 0.5 T superconducting scanner (Technicare). Multiple-section axial views using spin-echo (SE) technique with echo time (TE) of 30 msec and repetition time (TR) of 500 msec (SE 30/500) (T1-weighted) and with SE 90/1500 or 2000 (T2-weighted) were obtained routinely in all patients. Single- or multiple-section sagittal

Received February 12, 1985; accepted after revision May 14, 1985.

[1] Department of Radiology, New York Hospital–Cornell Medical Center, New York, NY 10021.

[2] Present address: Department of Radiology, University of California, Davis Medical Center, 4301 X St., Sacramento, CA 95817. Address reprint requests to B. C. P. Lee.

AJNR 6:863–870, November/December 1985
0195–6108/85/0606–0863

TABLE 1: **MR, CT, and Angiographic Findings in Cerebral Vascular Malformations**

Case No., Location	MR Imaging				CT			Angiography
	Malformation		Hematoma	Brain	Enhancement	Increased Attenuation	Brain Attenuation	
	SE 30	SE 90		SE 90				
1, Frontotemporal	D	D	Yes	I	Vascular	Blood	D	AVM
2, Frontotemporal	D	D	Yes	I	Vascular	Blood	D	AVM
3, Temporal	D	D	Yes	I	Nonspecific	Nonspecific	N	AVM
4, Temporal	D	D	No	N	Vascular	No	N	AVM
5, Frontoparietal	D	D	No	N	Vascular	No	N	AVM
6, Parietal	D	D	No	I	Vascular	No	N	AVM
7, Frontal	D	I	No	N	Vascular	No	N	Venous
8, Frontoparietal	D	I	No	N	Vascular	No	N	Venous
9, Cerebellum	D	N	No	N	Vascular	No	N	Venous
10, Cerebellum, brainstem	D	I	No	I	Vascular	N	N	Venous
11, Pons, midbrain	D,W	...	Yes	N	Nonspecific	Nonspecific	N	Negative
12, Pons	D,A/W	...	Yes	N	Nonspecific	Nonspecific	N	Negative
13, Pons	D,A/W	...	Yes	N	Nonspecific	Nonspecific	N	Negative
14, Pontomedullary	D,A/W	...	Yes	N	Nonspecific	Nonspecific	N	Negative
15, Pons	D,W	...	No	N	Nonspecific	Calcium	N	Negative

Note.—D = decreased; I = increased; N = normal; A = around; W = within.

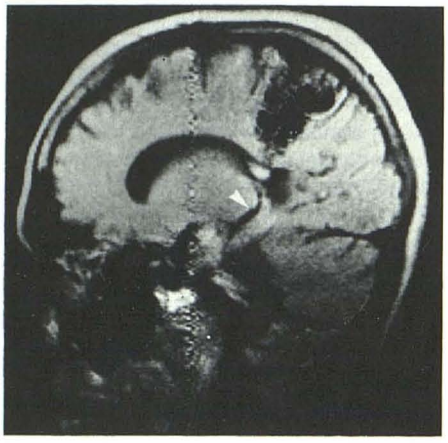

Fig. 1.—Sagittal SE 30/500 image. AVM is seen as serpiginous region of absent signal. Enlarged vein draining into deep venous system (*arrowhead*). Angiographic diagnosis: AVM.

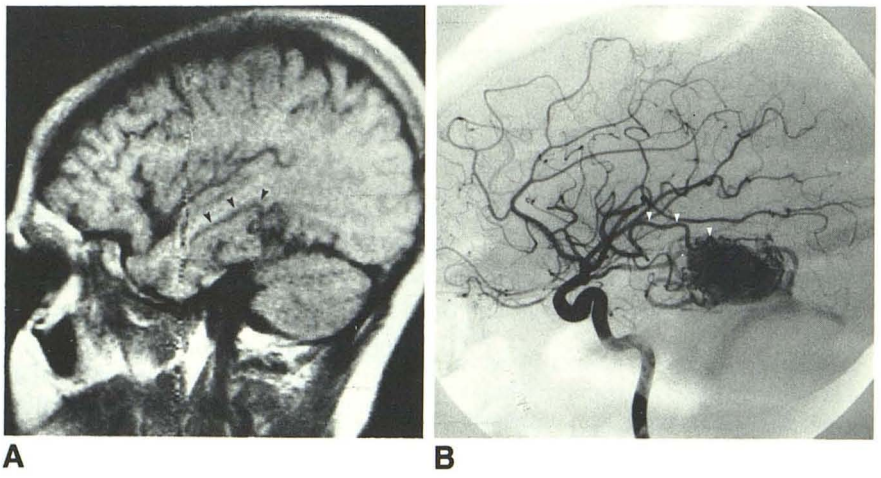

A B

Fig. 2.—**A**, Sagittal SE 30/500 scan. Malformation supplied by temporal branch of middle cerebral artery (*arrowheads*). **B**, Lateral angiogram confirms arterial supply (*arrowheads*). Angiographic diagnosis: AVM.

sections using SE 30/500 were also obtained routinely. Additional sections in either plane using SE 120/1500, 2000 or inversion-recovery (IR) techniques were obtained in selected cases. The thickness of the sections was 8 mm for multiple and 10 mm for single sections. All multiple sections were noncontiguous, with gaps of the same thickness as the sections; the intervening spaces were demonstrated by rescanning with spatial offsets identical to the slice thickness. The spatial resolution of the sections was 1.2–1.5 mm.

CT scans were obtained using a GE 8800 or 9800 scanner, before and after administration of a single dose of intravenous contrast material. Supratentorial lesions were examined with 10-mm-thick sections and posterior fossa lesions by 5-mm-thick sections.

Subtraction angiography was performed in all cases: one patient with malformations in the cerebral hemisphere and brainstem developed a seizure in the course of the test injection, necessitating termination of the procedure. Four hemispheric and two brainstem malformations were surgically verified.

Criteria for Evaluating Scans

The presence of abnormal vessels, hemorrhage, and abnormal signal in the malformation and adjacent brain parenchyma were determined on MR scans. Contrast enhancement of abnormal vessels, increased attenuation of blood and calcium, and low attenuation of brain adjacent to malformations were assessed on CT scans.

Results (table 1)

Arteriovenous Malformations (AVMs)

The six AVMs were visible on MR as an area of absent signal on both T1-weighted (SE 30/500) and T2-weighted (SE 90/1500, 2000) images in all six cases (fig. 1). Individual vessels were seen as serpiginous structures: arteries were of small caliber (fig. 2) and distinguishable from draining veins,

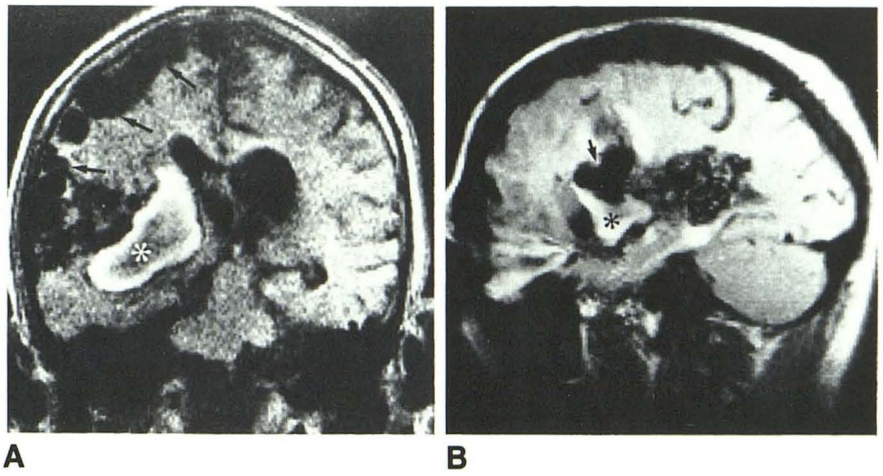

Fig. 3.—Coronal SE 30/500 scan. Large-caliber vein draining AVM (*arrows*). Hemorrhage (*). **B**, Sagittal view (another case). Aneurysmal dilatation of draining vein (*arrow*). Angiographic diagnosis: AVM.

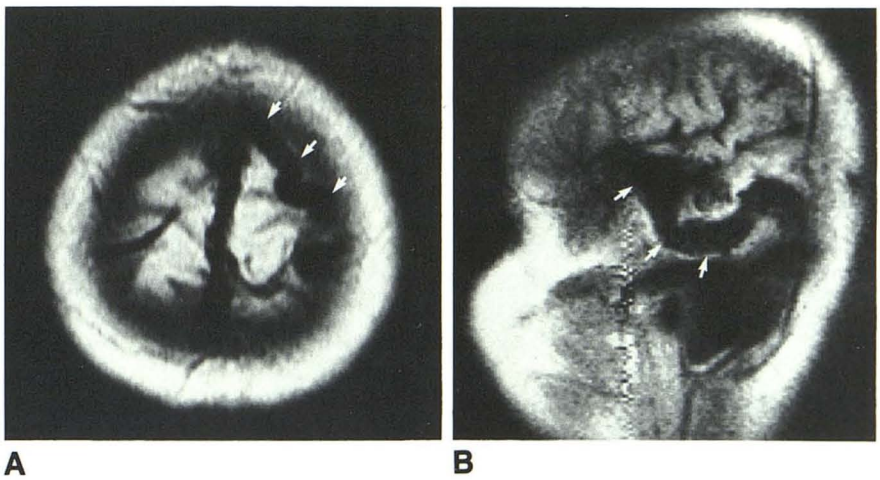

Fig. 4.—**A**, Axial SE 30/500 scan. Cortical vein (*arrows*) draining into sagittal sinus. **B**, Sagittal SE 30/500 scan. Another vein (*arrows*) draining into lateral sinus. Angiographic diagnosis: AVM.

which were larger (figs. 3 and 4). The arterial branches supplying the malformations were precisely demonstrated in two cases (fig. 2). Contrast-enhanced CT demonstrated the abnormal arteries in five cases but did not identify the precise origins of the branches supplying the malformations. Veins draining into the deep venous system were demonstrated; cortical veins were poorly defined in five cases. In one case with hemorrhage the enhancement was nonspecific and did not have characteristics to indicate the vascular origin of the lesion. All six AVMs were demonstrated on cerebral angiography.

Hyperintense signal in both T1-weighted (SE 30/500) and T2-weighted (SE 90/1500, 2000) images was shown in three cerebral AVMs and was consistent with hemorrhage: the hemorrhages were intraparenchymal in two cases and intraparenchymal as well as intraventricular in one case (figs. 5 and 6). CT confirmed hematoma in the same cases.

Hyperintense signal was seen on T2-weighted (SE 90/1500, 2000) images within and adjacent to AVMs that had bled in three cases and in another case without evidence of hemorrhage (figs. 5 and 7). CT showed decreased density adjacent to the hemorrhage in two cases; the density was normal in the other two cases.

Venous Malformations

In the three patients with venous malformations, the abnormal veins were visible as curvilinear structures without signal on T1-weighted (SE 30/500) images in two cerebral and in one cerebellar hemisphere malformations. These veins had increased signal on T2-weighted (SE 90/1500, 2000) images in two cases (fig. 8). Contrast-enhanced CT demonstrated abnormal veins in all cases, but not as clearly as on MR. Some veins were seen on MR but not on CT. All venous malformations were confirmed on cerebral angiography (fig. 8). No hematoma or abnormal signal on T2-weighted (SE 90/1500, 2000) images was shown in brain parenchyma in cases of venous malformation.

Locations of the Malformations

Two AVMs were located in the frontotemporal region, one in the frontoparietal area, two in the temporal region, and one

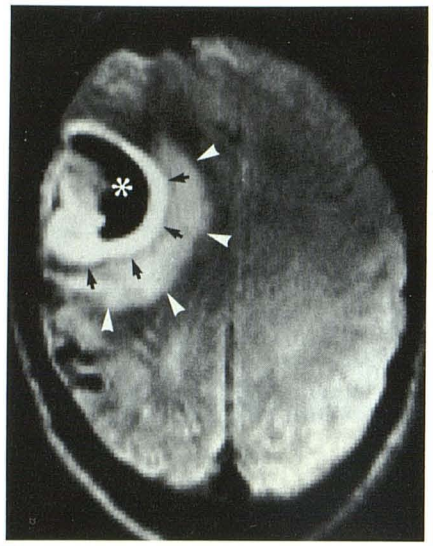

5

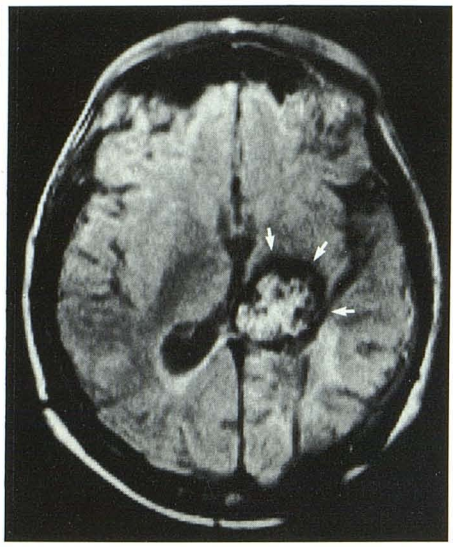

6

Fig. 5.—Axial SE 90/1500 scan. Area of increased signal compatible with hematoma (*arrows*). Less intense increased signal (*arrowheads*) adjacent to AVM. Lumen of vessels lacks signal due to flowing blood (*). Angiographic diagnosis: AVM.

Fig. 6.—Axial SE 90/2000 scan. Increased signal in malformation due to hemorrhage and absence of signal in vessels around hemorrhage (*arrows*). Postoperative changes in occipital region. Angiographic diagnosis: AVM.

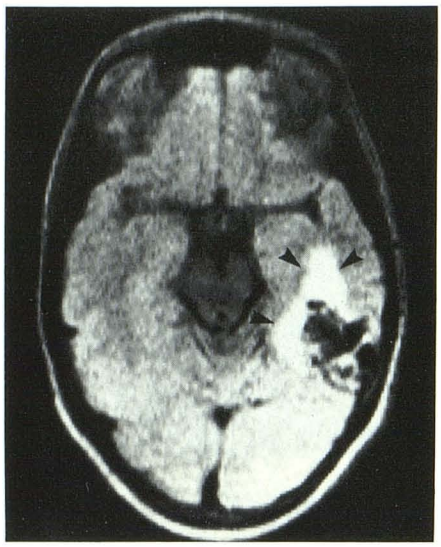

A

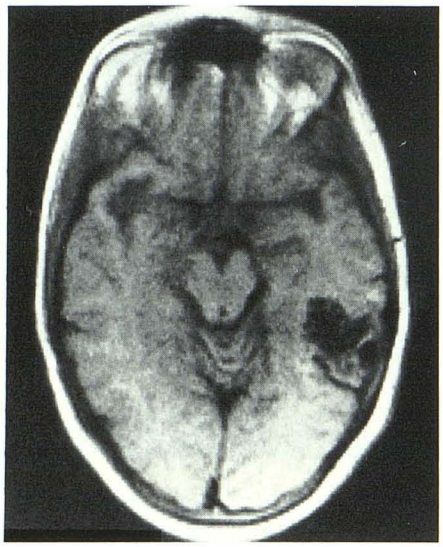

B

Fig. 7.—**A**, Axial SE 90/1500 scan. Increased signal in brain parenchyma (*arrowheads*) adjacent to AVM. **B**, SE 30/500 scan. No evidence of hemorrhage. Angiographic diagnosis: AVM.

in the parietal lobes (fig. 9). The three venous malformations were situated in the frontal region, the frontoparietal area, and the cerebellar hemisphere.

Brainstem Vascular Malformations

Of the six brainstem malformations, hyperintense signal consistent with hemorrhage was shown within the brainstem on T1-weighted (SE 30/500) and T2-weighted (SE 90/1500, 2000) images in four. Multiple areas of decreased signal were demonstrated within the hematomas in all these cases; a curvilinear decreased signal was shown around the hematomas in three cases (fig. 10). In a further case a similar low signal was shown by the same techniques without an associated hematoma (fig. 11). The brainstem was enlarged only when a hematoma was present. CT demonstrated increased attenuation in all five cases: the appearance and attenuation value were consistent with calcification in one case (fig. 11A); the values in the other cases were not specific for hemorrhage or calcification. Angiography was normal in all five cases.

In one case linear strands of hypointense signal were shown within the brainstem on SE 30/500 scans. The same regions became hyperintense on SE 90/2000. CT demonstrated a linear band of enhancement within the brainstem and brachium pontis. Angiography revealed a venous malformation with several abnormal veins within the pons and cerebellum (fig. 12).

Discussion

Intracerebral vascular malformations are divided histologically into true AVMs, cavernous malformations, telangiectasis,

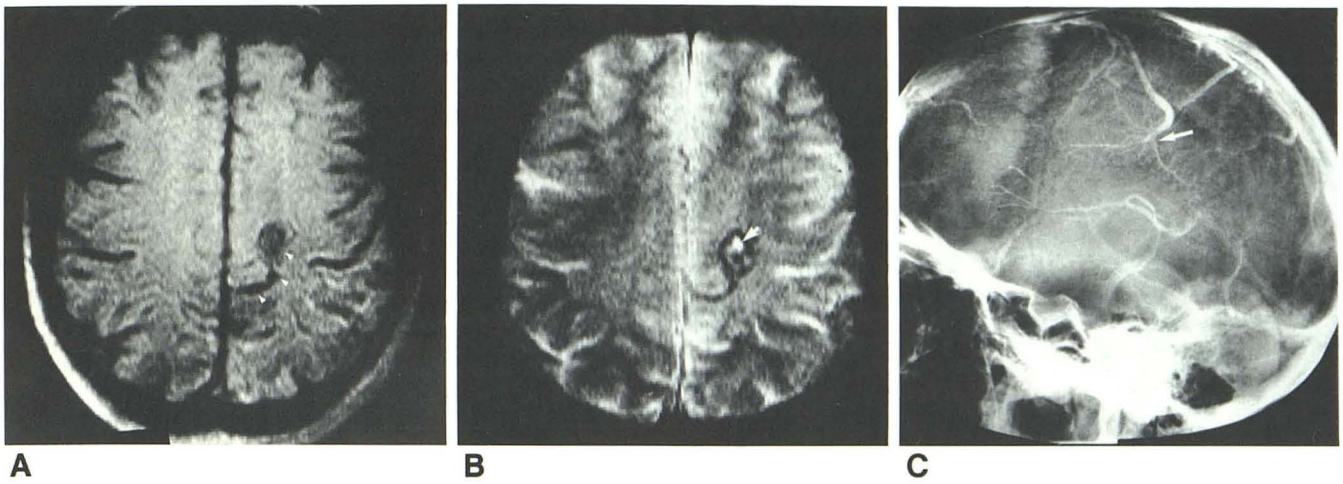

Fig. 8.—**A**, Axial SE 30/500 scan. Curvilinear region of poor signal (*arrowheads*). **B**, SE 90/1500 scan. Increased intensity of center (*arrow*). **C**, Lateral angiogram confirms venous malformation (*arrow*).

Fig. 9.—Sagittal SE 30/500 scan shows precise location of malformation in relation to sylvian fissure (*arrowheads*). Hemorrhage. Angiographic diagnosis: AVM.

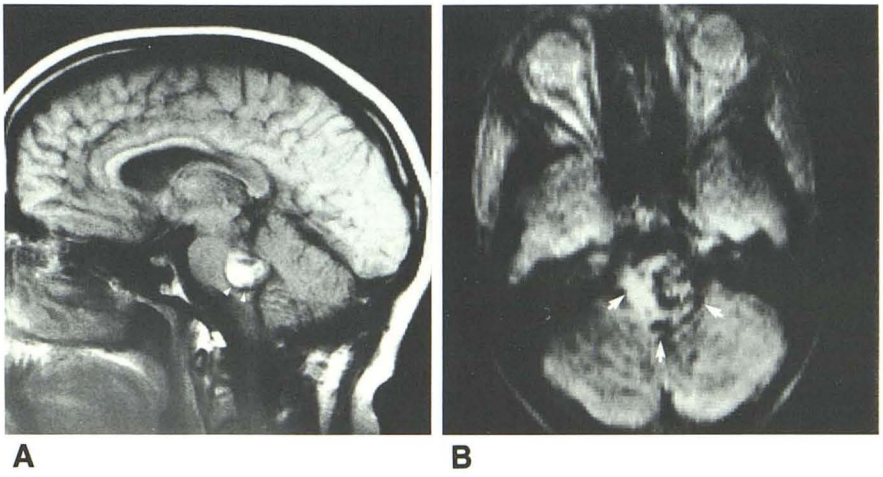

Fig. 10.—**A**, Sagittal SE 30/500 scan. Increased signal compatible with hematoma and multiple areas of lack of signal within and surrounding hematoma (*arrowheads*). **B**, Axial SE 90/1500 scan (another case). Similar appearances (*arrows*). Vascular malformation (negative angiogram).

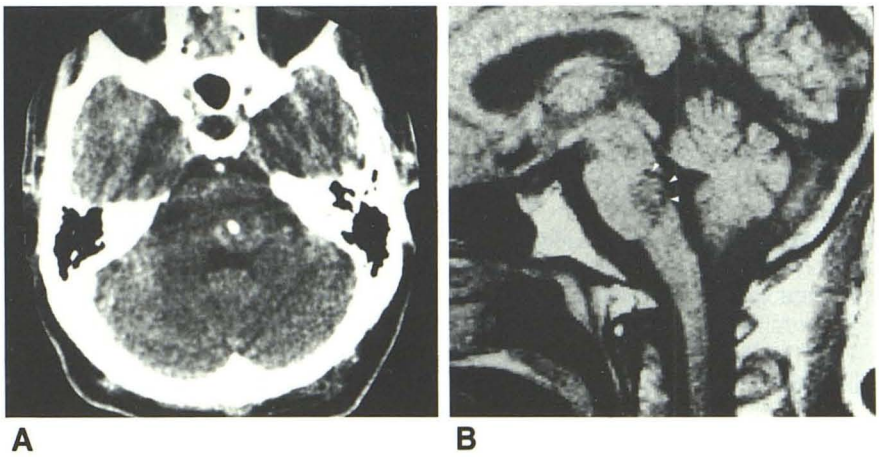

Fig. 11.—**A**, Unenhanced CT scan. Slight enlargement of left brachium pontis, with compression of fourth ventricle. Areas of increased attenuation had values of calcium. **B**, Sagittal SE 30/500 scan. Area of decreased signal surrounded by rim of low signal (*arrowheads*). Vascular malformation (negative angiogram).

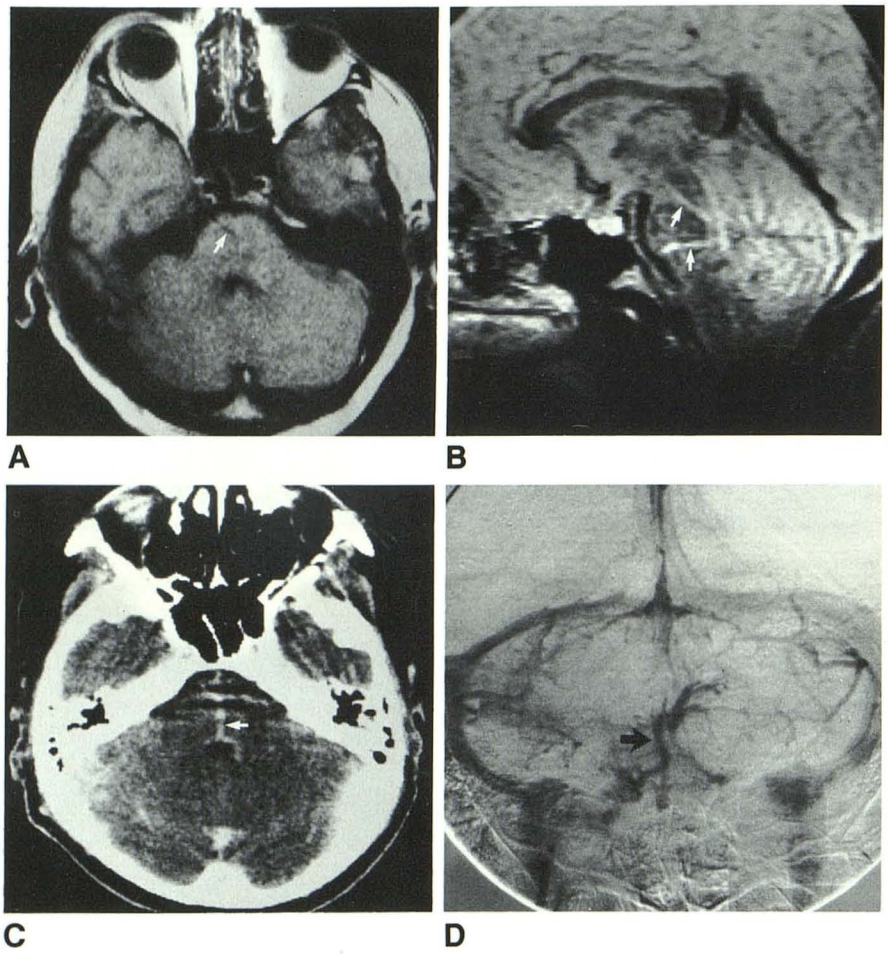

Fig. 12.—**A**, Axial SE 30/500 scan. Linear strand of decreased signal within pons extending to right side anteriorly (*arrow*). **B**, Sagittal SE 90/2000 scan. Multiple linear increased signal within pons and midbrain (*arrows*). **C**, Contrast-enhanced CT scan. Abnormal vessel traversing pons (*arrow*). **D**, Venous phase of angiogram confirms abnormal veins within brainstem and cerebellum (*arrow*). Angiographic diagnosis: venous malformation.

and venous malformations [19]. AVMs and venous malformations are consistently demonstrated by arteriography when the lesions have not bled [20–24], whereas cavernous and telangiectatic malformations are seldom visible angiographically [25–27]. The CT and MR appearances of AVMs and venous malformations are usually different from those of the other malformations.

AVMs

AVMs are commonly located in the cerebral and cerebellar hemispheres. Because of the rapid flow, the blood within the malformation and the feeding arteries and draining veins do not generate MR signal in any imaging sequence. The malformation itself is larger in size and more circumscribed than vessels that feed and drain it. The feeding arteries are sometimes delineated precisely on the lateral MR view, which demonstrates their relation with the normal branches of the anterior, middle, and posterior cerebral arteries. Draining veins are characterized by their caliber, which is larger than the arteries. Although veins draining into the deep venous system are effectively shown on CT, cortical veins are usually obscured by the calvaria. Such superficially situated veins are clearly delineated on MR, which is unaffected by such bone artifacts.

Hemorrhage is seen as well on MR as it is on CT. Hematoma older than 24 hr has homogeneous hyperintense signal on both T1- (SE 30/500) and T2- (SE 90/1500, 2000) weighted images, reflecting short T1 and long T2 relaxation times [28]. When the blood is organized the center has less signal. These appearances are sometimes helpful in determining the age of the hemorrhage. Discrete vessels are usually visible on contrast-enhanced CT in uncomplicated AVMs. Although contrast enhancement of the abnormal vessels is usually detected in the presence of hemorrhage, the enhancement often lacks the characteristic vascular configurations and may be difficult to differentiate from the enhancement of infarcts and tumors [3, 22, 23, 25, 27]. MR is probably more specific than CT in the diagnosis of AVMs since the abnormal vessels are usually seen clearly within areas of hemorrhage.

Cerebral tissue between and adjacent to vessels of the AVM are sometimes affected by anoxia, edema, or gliosis [1]. These changes are demonstrated dramatically on MR as hyperintense signal on T2-weighted (SE 90/1500, 2000) images and are more striking after hemorrhage. It is not possible to differentiate the exact nature of these abnormalities from

other causes of increased signal such as edema and tumor. The presence of similar abnormal signal in an AVM without hemorrhage suggests that the brain has been affected either directly by the malformation or by previous hemorrhage that has since resolved.

Venous Malformations

Venous malformations are usually smaller and have fewer vessels than AVMs [20, 24, 29]. The vessels shown on MR are less serpiginous than those of AVMs, and no discrete "malformations" are seen. The signal characteristics of the blood within the abnormal vessels are interesting in that no signal is seen when the TR is 500 msec or less, but signal is present and sometimes hyperintense when the TR is prolonged to 1500–2000 msec. These appearances suggest that the flow within the malformation is less rapid than that in true AVMs [17, 18]. The absence of hemorrhage and lack of abnormal MR finding in the brain parenchyma on T2-weighted images suggest that venous malformations do not affect normal brain tissue. It would be tempting to postulate that the absence of MR signal abnormality in the brain is in keeping with the more benign nature of venous malformations compared with AVMs [29].

Localization

Although axial and coronal CT sections are useful in locating AVMs in relation to the centrum semiovale and other normal deep structures, reformatted sagittal views have poor resolution. The precise anatomic locations of vascular malformations are best evaluated by MR with sagittal T1-weighted (SE 30/500) views, which invariably demonstrate the relation of the lesion to the normal sylvian fissure and cortical gyri and sulci.

Brainstem Malformations

Brainstem vascular malformations produce severe debilitating symptoms that may be indistinguishable from those of brainstem tumors [26, 27]. Telangiectasia or cavernous malformations are more common than true AVMs and venous malformations and are seldom demonstrated on angiography [25–27]. Although hemorrhage is a common presentation, it is usually difficult to differentiate from calcium by measurement of CT attenuation values alone [27, 30]. MR is much more precise than CT in identifying a hematoma that is not fresh (first 1 or 2 days) because of the characteristic increased signal reflecting short T1 and long T2 relaxation times. The regions of absent signal within and surrounding a hematoma may represent vessels of the malformation or a pathologic process in the brain. The combination of an enlarged brainstem due to a hematoma and such regions of decreased signal peripheral to the hematoma favors the diagnosis of a vascular malformation. Unlike vascular malformations, brainstem gliomas seldom produce hemorrhage, and the signal of the tumor is usually hypo- or isointense on T1-weighted (SE 30/500) images, becoming hyperintense on T2-weighted (SE 90/1500, 2000) images. Abnormal vessels are also seldom seen on MR scans [31].

Occasionally vascular malformations are not accompanied by hemorrhage, and the brainstem is not enlarged. The configuration of the abnormal vessels, which lack signal, may be helpful in differentiating malformations from brainstem neoplasms. Rarely, blood within brainstem vascular malformations shows increased signal on SE techniques using long TEs and TRs. This presumably reflects sluggish flow, which is more common in venous malformations than in true AVMs.

REFERENCES

1. Pool JL. Arteriovenous malformations of the brain. In: *Handbook of neurology*, vol 12. Amsterdam: North Holland, **1972**:266–277
2. Terbrugge K, Scotti G, Ethier R, Melancon D, Tcharg S, Milner C. CT in intracranial arteriovenous malformations. *Radiology* **1977**;122:703–705
3. Kramer RA, Wing SR. CT of angiographically occult cerebral vascular malformations. *Radiology* **1977**;123:649–652
4. Stein BM, Wolpert SM. Arteriovenous malformations of the brain: current concepts and treatment. *Arch Neurol* **1980**;37:1–5
5. Lussenhop AJ, Gennarelli TA. Anatomical grading of supratentorial arteriovenous malformations for determining operability. *Neurosurgery* **1977**;1:30–35
6. Drake CG. Cerebral arteriovenous malformations: consideration for and experience with surgical treatment in 166 cases. *Clin Neurosurg* **1979**;26:145–208
7. Giudetti B, Delitala A. Intracranial arteriovenous malformations: conservative and surgical treatment. *J Neurosurg* **1980**;53:149–152
8. Stein BM, Wolpert SM. Arteriovenous malformations of the brain. II. Current concepts and treatment. *Arch Neurol* **1980**;37:69–75
9. Fasane VA, Uriuoli R, Onzio RM. Photocoagulation of cerebral arteriovenous malformations and arterial aneurysms with the neodymium: yttrium-aluminum-garnet or argon laser. Preliminary results in 12 patients. *Neurosurgery* **1982**;11:754–759
10. Stein BM. Arteriovenous malformations of the medial cerebral hemisphere and the limbic system. *J Neurosurg* 1984;60:23–31
11. Luessenhop AJ, Rosa L. Cerebral arteriovenous malformations. *J Neurosurg* **1984**;60:14–22
12. Samson D, Ditmore M, Beyer CW. Intravascular use of isobutyl-2-cyanoacrylate. Part 1: treatment of intracranial arteriovenous malformations. *Neurosurgery* **1981**;8:32–51
13. Cromwell LD, Harris AB. Treatment of cerebral arteriovenous malformations: combined neurosurgical and neuroradiological approach. *AJNR* **1983**;4:366–368
14. Kjellberg RN, Hanamura T, Davis KR, Lyons SL, Adams RD. Bragg-Peak proton beam therapy for arteriovenous malformations of the brain. *N Engl J Med* **1983**;309:269–274
15. Steiner RE. The Hammersmith clinical experience with nuclear magnetic resonance. *Clin Radiol* **1983**;34:13–23
16. Brant-Zawadzki M, Davis PL, Crooks LE, et al. NMR demonstration of cerebral abnormalities: comparison with CT. *AJNR* **1983**;4:117–124, *AJR* **1983**;140:847–854
17. Singer JR, Crooks LE. Nuclear magnetic resonance blood flow measurements in the human brain. *Science* **1983**;221:654–656
18. George CR, Jacobs G, MacIntyre WJ, et al. Magnetic resonance signal intensity patterns obtained from continuous and pulsatile

flow models. *Radiology* **1984**;151:421–428
19. Russel DS, Rubinstein LJ. *Pathology of tumors of the nervous system*, 4th ed. Baltimore: Williams & Wilkins, **1977**:129–134
20. Fierstein SB, Pribram HW, Hieshima G. Angiography and CT in the evaluation of cerebral venous malformations. *Neurology* **1979**;17:137–148
21. Brunelle FOS, Harwood-Nash DCF, Fritz CR, Chuang SH. Intracranial vascular malformations in children: CT and angiographic evaluation. *Radiology* **1983**;149:455–461
22. Kamrin RB, Buchsbaum HW. Larger vascular malformations of the brain not visualized by serial angiography. *Arch Neurol* **1965**;13:413–425
23. Eisenman JI, Alckowmbides A, Pribram H. Spontaneous thrombosis of vascular malformations of the brain. *Acta Radiol* [*Diagn*] (Stockh) **1972**;13:77–85
24. Wendling LR, Moore JS, Kieffer SA, Goldberg HI, Latchaw RD. Intracerebral venous angioma. *Radiology* **1976**;119:141–147
25. Savioardo M, Strada L, Passerini A. Intracranial cavernous hemangiomas: neuroradiological review of 36 operated cases. *AJNR* **1983**;4:945–950
26. Roberson GH, Kase CS, Kolpow ER. Telangiectasis and cavernous angiomas of the brainstem: "cryptic" vascular malformations. *Neuroradiology* **1974**;9:83–90
27. Yeates A, Enzmann D. Cryptic vascular malformations involving the brainstem. *Radiology* **1983**;146:71–75
28. Bottomley PA, Foster TH, Raymond E, et al. A review of normal tissue hydrogen NMR relaxation times and relaxation mechanisms from 1-100 MHz: dependence on tissue type, NMR frequency, temperature, species, excision and age. *Med Phys* **1984**;11:425–448
29. Saito Y, Kobayashi N. Cerebral venous angiomas. *Radiology* **1981**;139:87–94
30. Zatz LM. Basic principles of computed tomography scanning. In: Newton TH, Potts DG, eds. *Radiology of the skull and brain: technical aspects of computed tomography*. St. Louis: Mosby, **1983**:3871–3872
31. Lee BCP, Kneeland JB, Walker RW, Posner JB, Cahill PT, Deck MDF. MR imaging of brainstem tumors. *AJNR* **1985**;6:159–163